THIELSCH ENGINEERING ASSOCIATES, INC.

195 Frances Avenue
Cranston, Rhode Island 02910
Tel. (401) 467-6454
Fax (401) 467-2398

CORROSION 91

The NACE Annual Conference and Corrosion Show
March 11-15, 1991 • Cincinnati Convention Center • Cincinnati, Ohio

PAPER NUMBER

244

ACCELERATED TUBE METAL WASTAGE IN MUNICIPAL SOLID WASTE FIRED FURNACES

W.G. Schuetzenduebel, I.E. Johnson and C.W. Clemons
Blount Energy Resource Corporation
4520 Executive Park Drive
Montgomery, AL 36195

H. Thielsch
Thielsch Engineering Associates, Inc.
195 Frances Avenue
Cranston, Rhode Island 02910

ABSTRACT

Accelerated tube metal wastage occurred in a municipal waste fired furnace prompting a study of the cause and remedial action required to prevent a recurrence. The study included a review of operating conditions, documentation of tube wall thinning, physical inspection of systems, metallographic examination of tubes and chemical analysis of tube scale utilizing Scanning Electron Microscopy and X-Ray Diffraction techniques. The high levels of tube metal wastage was attributed to fireside corrosive attack linked to a localized reducing atmosphere. The most likely cause of the localized reducing atmosphere was the buildup of a slag shelf over the secondary air nozzles, blocking flow, and preventing intimate mixing of air with products of combustion. Remedial efforts included tube repair, removal of slag deposits and changes in operating practices to minimize formation of localized reducing atmospheres. Tube repair was effected by replacement of a 3' x 3.5' tube wall section and an in-situ weld metal overlay of Alloy 625 (SFA - 5.14 ERNiCrMo-3) for added corrosion protection.

Keywords: waste-to-energy, boiler-tube failure, tube corrosion, wall thinning, tube scaling.

The failure of this tube in the No. 2 boiler was totally unexpected. Only 18 days prior to the failure, the No. 1 boiler had been given a thorough inspection and cleaning during a routine annual shutdown. The inspection included a survey of tube wall thicknesses using a KB ultrasonic thickness gauge. Measurements were taken throughout the furnace/boiler and compared with baseline readings taken shortly after initial start-up. Results showed practically no reduction in tube wall thickness. Following the tube failure in the No. 2 boiler, the No. 1 boiler was again subjected to a detailed tube wall thickness survey. Again, wall thickness deterioration was not apparent. How could it be that one boiler could experience metal wastage and tube failure while an identical boiler (same tube configuration, refractory, air supply and fuel) operating in parallel under similar operating conditions showed little or no signs of corrosion?

Believing there must be a fundamental explanation for this anomaly the investigation continued.

Physical Inspection of Furnace/Boiler Internals

Following the tube rupture, an internal inspection of both boilers was conducted. These inspections revealed a difference in slagging characteristics between the two units. Specifically, a large slag shelf was observed over the secondary air nozzles in the front wall of Unit No. 2, extending to as much as two feet into the furnace. Figure No. 4 is a photograph of this slag build-up. Also, differences in slagging of screen tubes and convection surfaces were observed between the two units. Unit No. 1 had the most severe slagging in the front sections with screen tubes plugged evenly over their length and slagging decreasing to virtually none in the economizer. Unit No. 2 had completely plugged screen tubes for the upper ten feet. Figures 5 and 6 are photographs of the slagging condition on the screen tubes and evaporator section, respectively, of Unit No. 2.

These observations led to the hypothesis that the most probable cause for accelerated corrosion attack may be sought in a reducing flue gas atmosphere. Such reducing atmosphere can be attained by incomplete combustion resulting from localized air starvation, incomplete gas/air mixing or gas recirculation. The fact that the corrosion took place on both side walls and the front wall close to both corners, and in view of the fact that a massive slag build-up over the secondary air nozzles was present, lead to the conclusion that a local starved air condition may have existed in the areas of highest corrosion.

LABORATORY EXAMINATIONS

Tube samples from the failed area of the front wall were submitted to Thielsch Engineering Associates, Inc. for examination and testing. Figure 7 is a photograph of the tube samples submitted which included the failed tube denoted as tube No. 12.

Visual examination showed severe wall thinning in the failed tube. In addition, the fireside of the failed tube and other adjacent tubes had a very rough texture, typical of fireside corrosion.

A dimensional sketch was prepared to document the wall thinning in the failed tube and in the adjacent tubes. Results are shown in Figure 8. It was noted that the loss of wall thickness in all tubes examined had occurred from the outside diameter of the tubes and was most severe along the fireside crown. The wall thickness at the failure location was 0.022 inches, representing a reduction of 87% from the original wall thickness as recorded along the cold side of the tube.

Metallographic Examination

To determine if the corrosion problem was associated with overheating or was a low temperature phenomenon, two cross sections were cut from representative locations. Subsegments were removed from these cross sections at 0° (fireside) and 180° (coldside), mounted in bakelite, surface ground, polished and etched using a 2% Nital solution. They were then examined at higher magnifications and representative locations were selected for documentation.

Cross Section "A-A." Tube No. 12 was cross-sectioned through the leak location at "A-A", as indicated in Figure 9. The subsegments removed are shown subsequent to metallographic preparation at a magnification of 1X in Figure 10. Rockwell "B" hardness determinations were made at the locations shown. Corresponding Brinell hardness numbers, provided in ( ), ranged from 89 BHN to 98 BHN. This extrapolates to a tensile strength of 45,000 psi. This is slightly low for tubing produced in accordance with ASME Specification SA-178, Grade A, but is still considered acceptable.

As mentioned, these subsegments were examined comprehensively and representative locations were selected for documentation.

These locations, identified as "A_2" to "A_5" are indicated on the photomacrographs (magnification 10X) supplied in Figure 11.

Area "A_2", located at the fracture surface, is shown at magnifications of 100X and 500X in Figure 12. The microstructure at this location consisted of ferrite and lamellar pearlite. The grains of each constituent showed straining and also elongation as a result of the rupture.

Area "A_3", located at the mating fracture surface, is shown in Figure 13. Intergranular attack was evident along the outside surface. This is typical of a corrosion associated phenomenon. The microstructure was similar, comprised of ferrite and lamellar pearlite. The presence of lamellar pearlite is indicative that this tube was not subject to overheating.

Areas "A_4" and "A_5", located along the outside and inside diameter surfaces of the 180° subsegment, are shown in Figures 14 and 15 respectively. The microstructure was typical, comprised of ferrite and lamellar pearlite. There was little or no scale formation. This is also indicative that the tube had not been subject to overheating.

Cross Section "B-B." Cross section "B-B" was cut through tube No. 11 at the elevation corresponding to the leak location in Tube 12 (reference Figure 9). It is shown subsequent to metallographic preparation at a magnification of 1X in Figure 16. Rockwell "B" hardness determinations were made at the locations shown.

Brinell hardness numbers are provided in ( ). The hardness values recorded ranged from 98 BHN to 99 BHN and are considered acceptable.

Photomacrographs of the subsegments, provided in Figure 17, document the severe reduction in wall thickness at the 0° side. The minimum wall thickness measured 0.020". This represents 12.5% of the original wall thickness (0.160") recorded on the 180° side, ie., an 87.5% loss of the original wall thickness.

The microstructure observed in these subsegments is documented at higher magnifications in Figures 18 through 20. It was similar to that observed previously, comprised entirely of ferrite and lamellar pearlite. There was minimal scale formation observed, again confirming that these tubes were not subject to overheating.

Chemical Analysis

Subsequent to the metallographic examination of the tubes, a small segment was removed from sample No. 12 and qualitatively analyzed by Optical Emission Spectroscopy (OES) to confirm the material grade. The results were as follows:

Element	Sample 12 (wt./%)	ASME SA-178 Gr.A (wt./%)
C	0.12	0.06 - 0.18
Mn	0.38	0.27 - 0.63
P	0.018	0.05, max.
S	0.004	0.06, max.
Si	0.015	-

The tubes were produced in accordance with ASME Specification SA-178, Grade A. They are in compliance with this specification.

Scanning Electron Microscopy

To determine what contaminants were involved in the corrosive attack, the scale along the outside diameter of the tubes was qualitatively analyzed by Scanning Electron

Microscopy (SEM) in conjunction with Energy Dispersive Spectroscopy (EDS). A scanning electron micrograph at location "C" (reference Figure 9) is provided in Figure 21. An energy dispersive spectral plot recorded at this same location is provided in Figure 22. Sulfur and chlorine peaks were observed. In addition, trace quantities of potassium and zinc were noted. Under the operating conditions involved, all four of these elements can cause extensive problems, particularly the presence of significant quantities of sulfur and chlorine.

X-Ray Diffraction

The surface scale was also analyzed for composition by X-Ray Diffraction.

The majority (approximately 70%) of the scale scraped from the tube was noncrystalline, and therefore, its composition could not be determined. The remaining scale was determined to be hematite (Fe_2O_3) and magnetite (Fe_3O_4). Hematite, or rust, is a scale which forms at low temperatures.

Magnetite forms at or above 500°F. Small quantities of free iron were also noted in the scale. These results are not typical of a tube under normal operating conditions.

The large quantity of noncrystalline oxide indicates that the scale which formed on the tube is not resistant to mechanical damage. This is typical of a sulfide or chloride based scale, rather than an iron based scale.

Discussion of Laboratory Results

The loss in wall thickness in the tubes in the Unit No. 2 furnace is associated with a corrosive attack linked to a localized reducing atmosphere in the furnace. The reducing atmosphere is associated with incomplete combustion which may result from localized air starvation or incomplete gas air mixing.

Under these conditions, i.e., a reducing atmosphere, sulfur in the fuel is released mostly as H_2S. This deposits on the tube surfaces, destroying the original oxide and resulting in the formation of a new sulfide-based scale. These sulfides are not as protective as the original iron oxide layer. Several reasons are applicable: they are not as tightly adherent, they are not as resistant to mechanical damage, and they are less resistant to mass transport than the original oxide coating.

As a result, these coatings allow for rapid attack of the tube metal, particularly when incompletely oxidized furnace gases contact the furnace wall or when unburned combustibles impinge the furnace wall.

This situation is further aggravated by the presence of chlorides. Chlorine will form HCl which will in turn combine with the original protective iron oxide layer forming $FeCl_2$. This will increase the porosity of the scale, thereby reducing its protective characteristics. Thus, chlorine will further accelerate the sulfidation corrosion.

REMEDIAL ACTIONS

Tube Wall Repair

The immediate task at hand following the tube failure in the No. 2 Unit was to affect repairs and bring the unit back on line. To determine the extent of the problem, a detailed ultrasonic wall thickness survey was performed over the three waterwall sections in the furnace. Readings were taken commencing at the top of the refractory lined zone and extending to a distance of 6' - 6" above the refractory. It was concluded from these data that tube wall thinning was occurring on three furnace walls with severest thinning on the west wall where the tube rupture occurred (see Figure 2).

Three options for repair were deemed available: a) replacement of affected tubes with original carbon steel tubes b) replacement with alloy tubes or c) overlay of existing carbon steel tubes with a corrosion resistant alloy material.

Replacement with original carbon steel tubes offered the lowest first cost solution but provided no assurance of repeat failures. Replacement with alloy tubes offered good assurance against repeat failures but would be extremely expensive and require a lengthy shutdown. The repair mode selected was to overlay the tubes in-situ with a weld metal buildup using Alloy 625 (SFA - 5.14 ERNiCrMo - 3). The overlay consisted of an eight foot band starting at the top of the refractory and was applied to all three walls.

Prior to the overlay, it was necessary to remove and replace a section of the wall tubes since a minimum of 0.070 inch wall was required in order to minimize blow-through while weld-overlaying. The area replaced measured approximately 3 ft. high and 3 ft. - 6 in. long.

The resulting boiler tube wall thickness after weld overlay was between 0.250 inches and 0.300 inches.

Operating Practice

Several modifications to plant operating practices were instituted to improve operations and minimize the possibility of local reducing atmospheres in the furnace. Among the more important strategies were:

- More frequent observation of firing conditions on the grate to detect smoldering fires, overloaded grate sections, incomplete combustion, grate section failures, air problems etc.
- Frequent inspections to detect slagging, particularly in the areas surrounding the secondary air nozzles to assure unobstructed full air flow and to record progression of slag buildup.
- Increased surveillance of the condition of boiler tube rappers and components and a requirement to make immediate repairs to defective parts.

SUMMARY

The corrosive attack in the tubing in the Unit No. 2 boiler at the Warren Energy Resource Company facility in Oxford, New Jersey is associated with localized reducing atmospheres. Such localized reducing atmosphere, in conjunction with sulfur and chlorine found in the fuel, result in accelerated corrosion along the fireside of the tubes.

The most probable cause of the localized reducing atmosphere in Unit No. 2 was the build-up of a large slag shelf over the secondary air nozzles which restricted air flow and prevented adequate mixing of combustion products and air.

Remedial efforts included tube repair, removal of slag deposits and changes in operating practices to minimize formation of localized reducing atmospheres. Tube repair was affected by replacement of a 3' x 3.5' tube wall section and an in-situ weld metal overlay of alloy 625 (SFA - 5.14 ERNiCrMo - 3) for added corrosion protection.

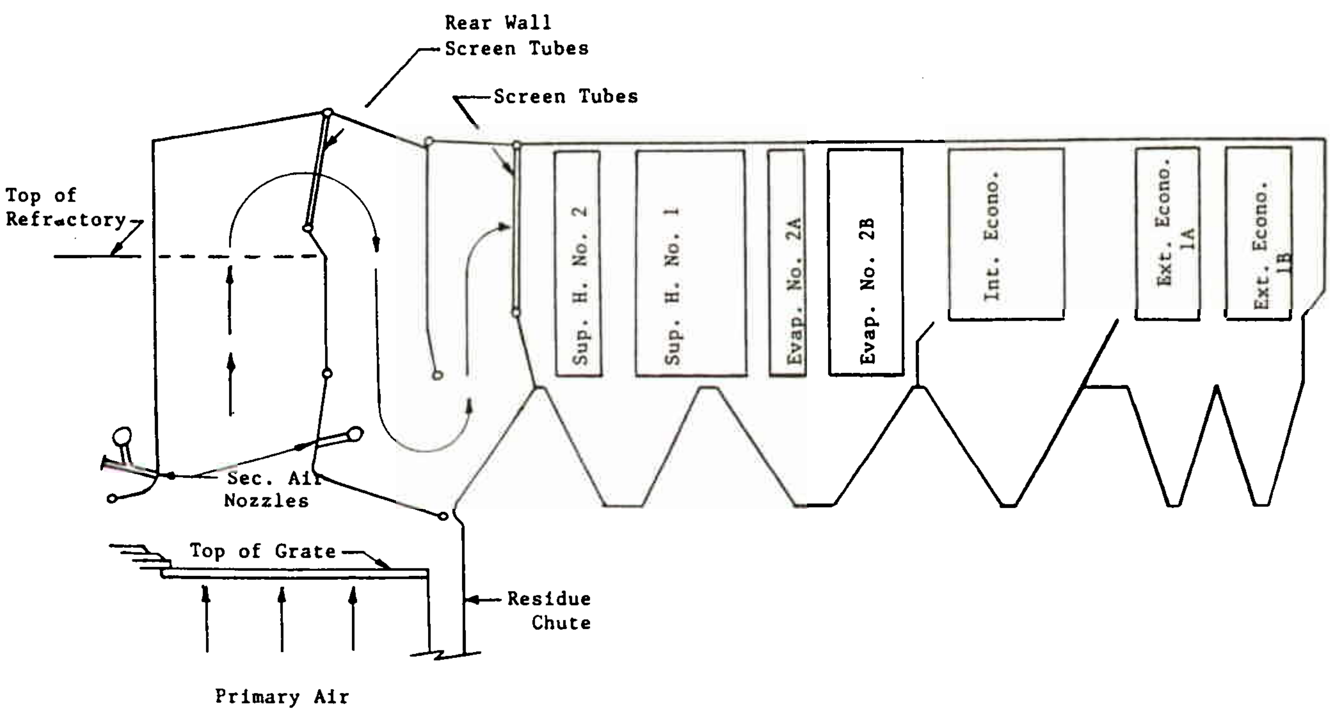

Figure 1. Boiler Cross Section Schematic.

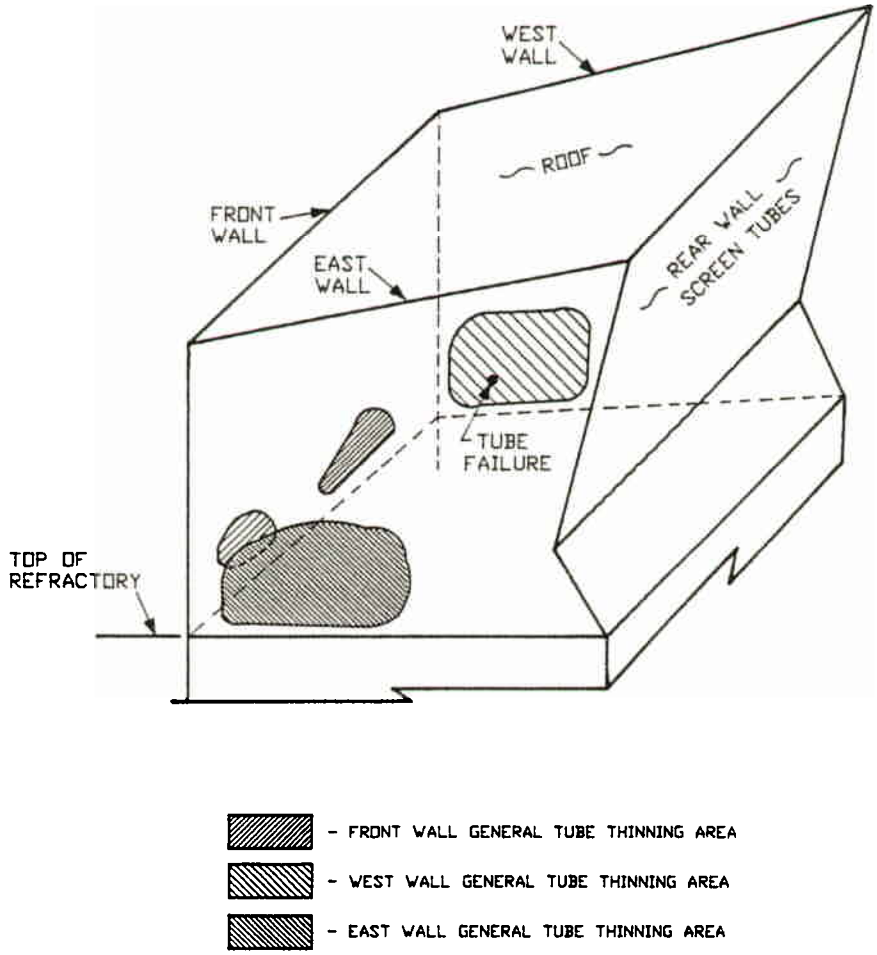

Figure 2. Furnace Gas Passage Schematic.

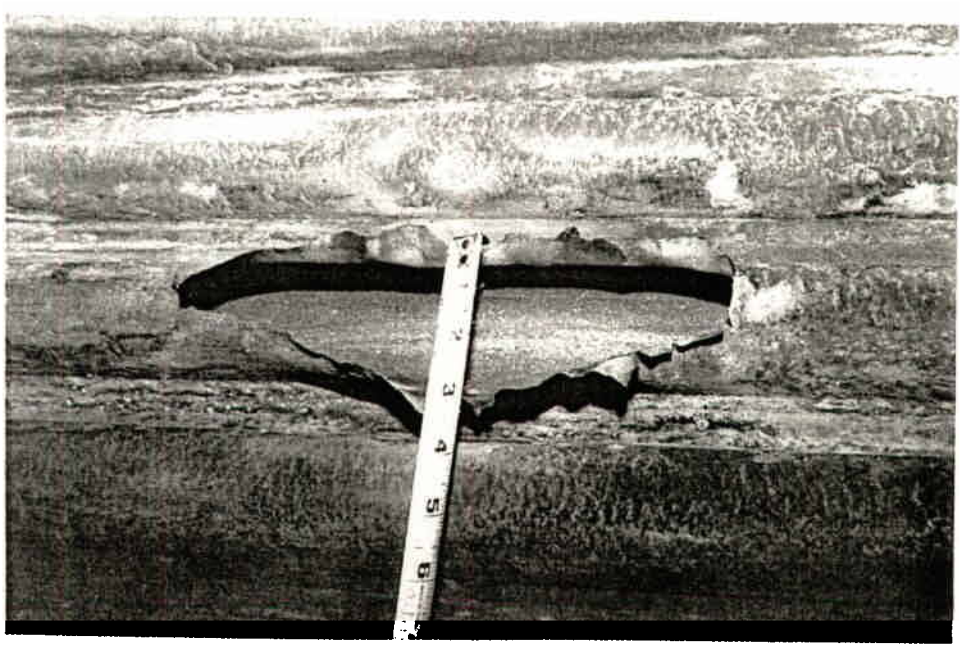

Figure 3. Photograph of Failed Tube.

Figure. 4. Slag Build-up Over Secondary Air Nozzles.

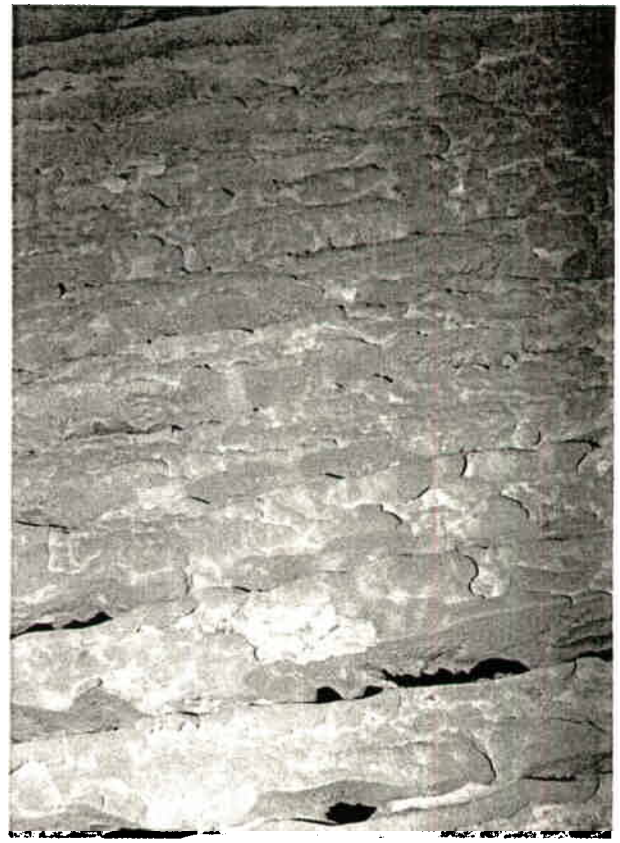

Figure 5. Screen Tube Slagging Condition.

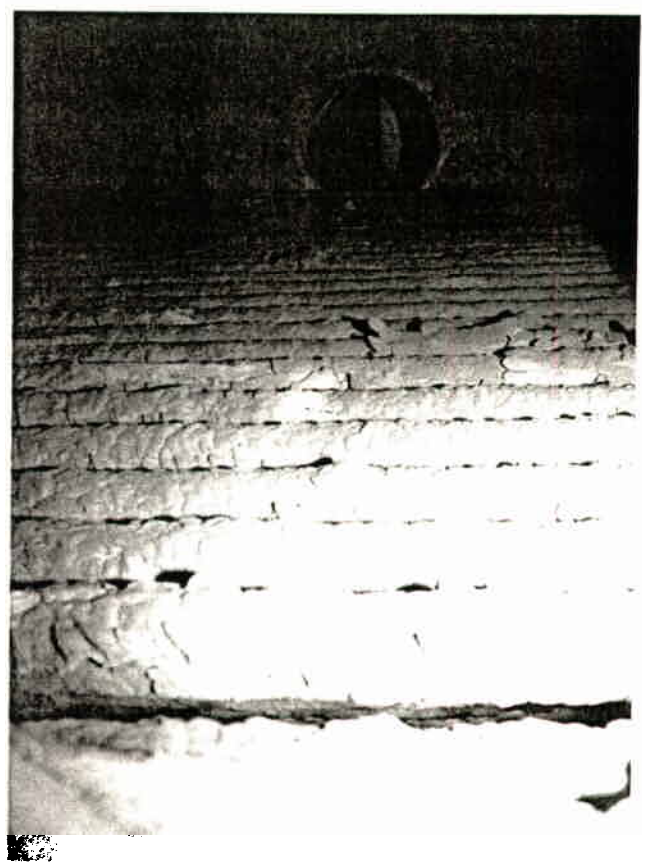

Figure 6. Slagging Condition of Evaporation bundle Tubes.

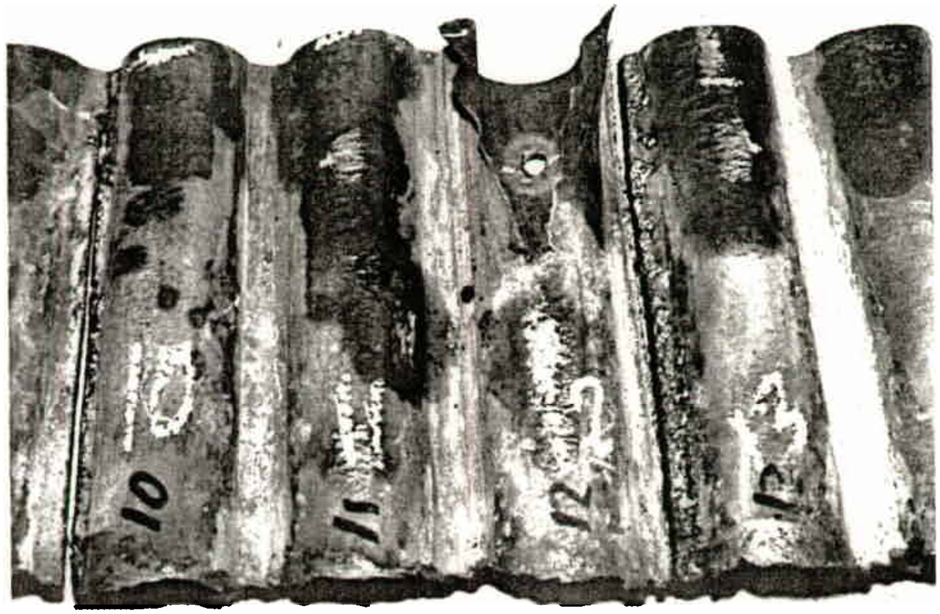

Figure 7. Overall View of Tube Panel
Examined.

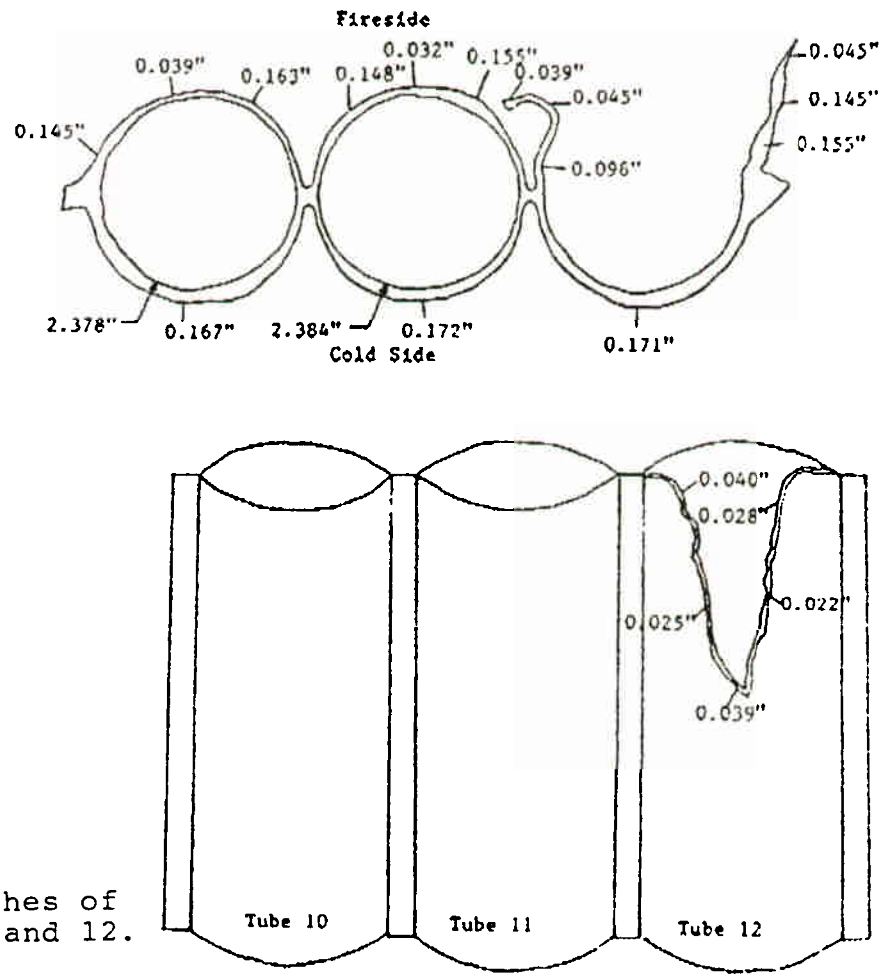

Figure 8. Dimensional Sketches of
Tubes Nos. 10,11 and 12.

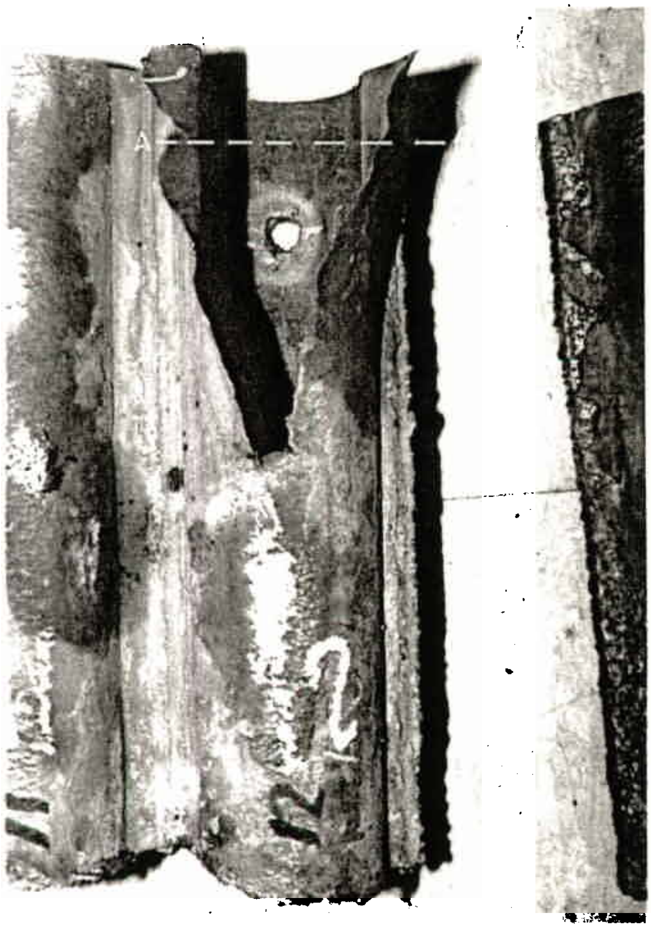

A

B

Figure 9. Close-up Views of Failure Locations(1/2X).

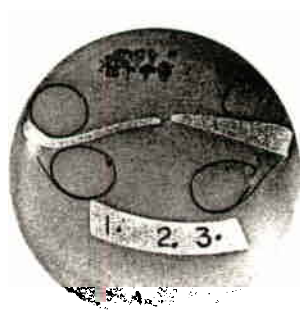

Figure 10. Overall view of Cross Section "A-A". Rockwell B. Hardness Determinations Are Also Provided. Brinell Values Are Shown in ( ).

1. 53.0 (98)
2. 53.1 (98.2)
3. 49.0 (89.0)

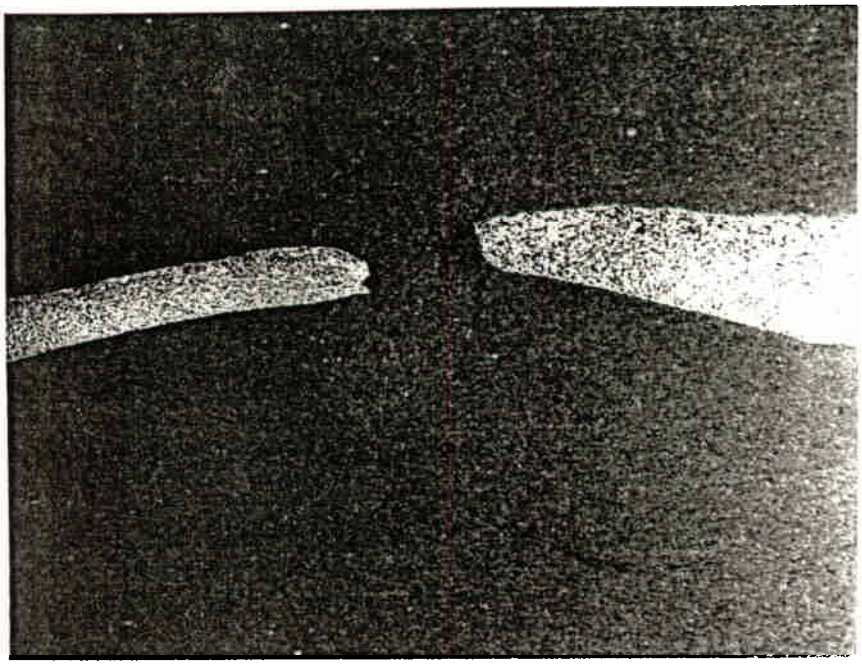

A

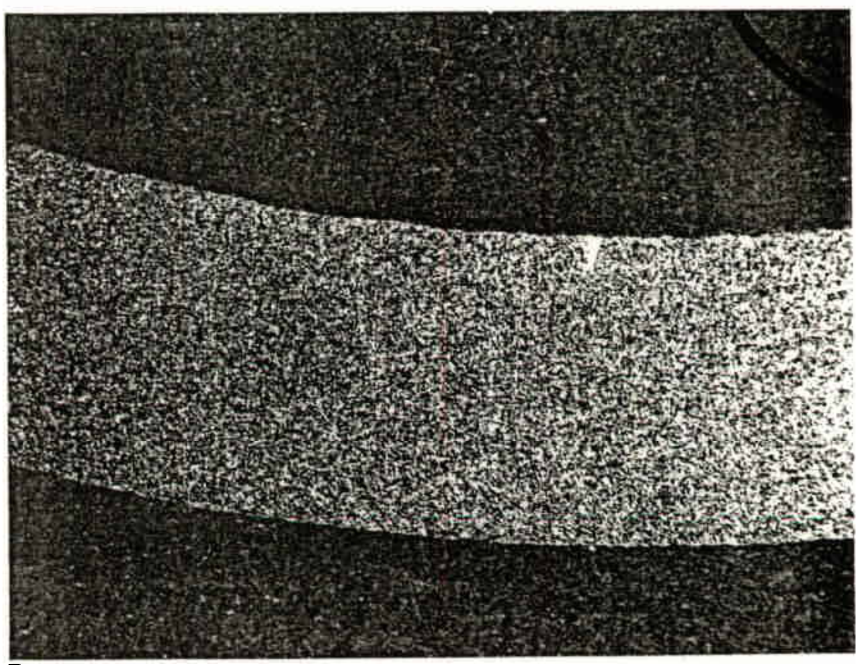

B

Figure 11. Photomacrograph of Cross Section "A-A".

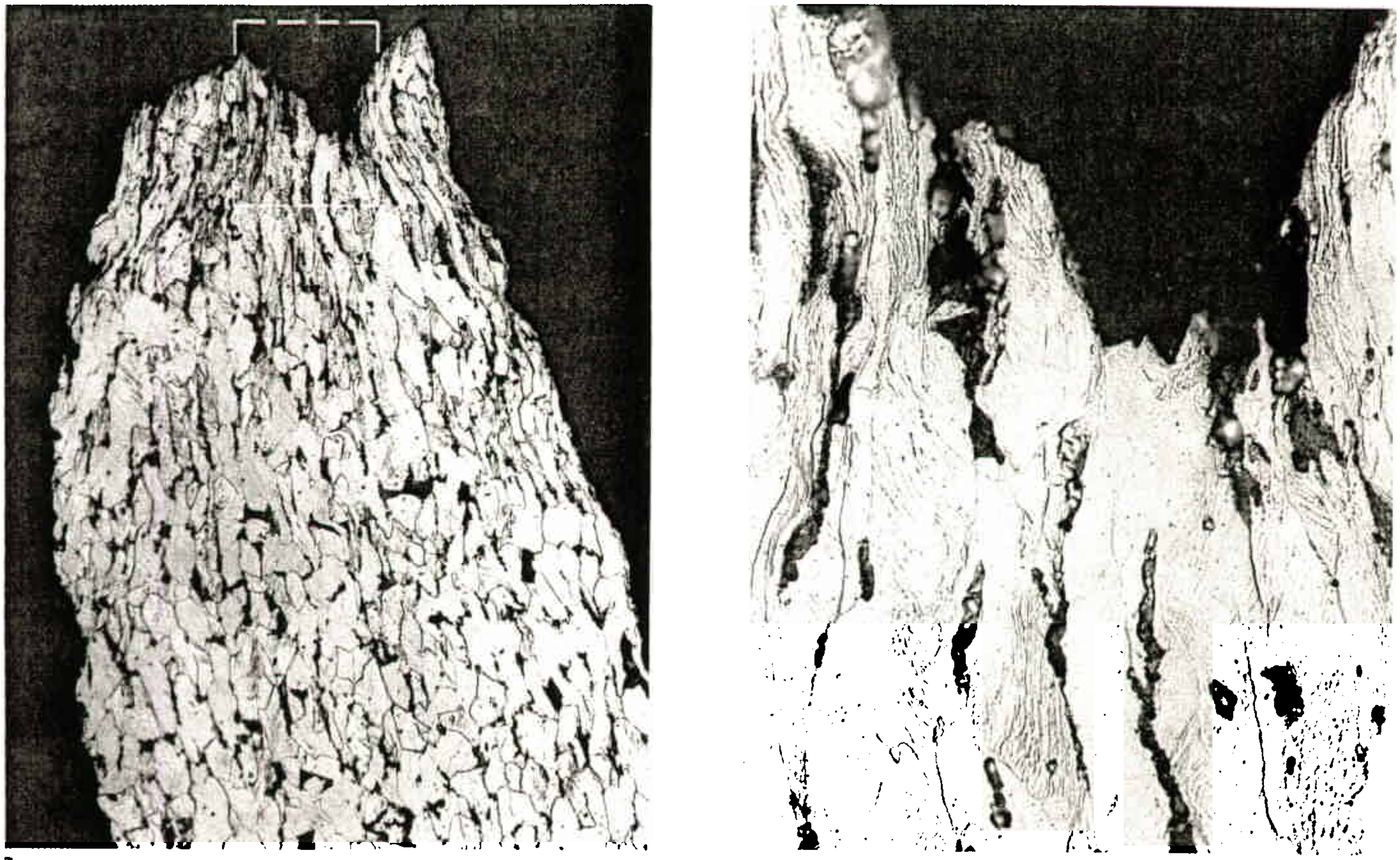

A B

Figure 12. Microstructure At "A_2" (100X) (500X).

A B

Figure 13. Microstructure At "A_3" (100X) (500X)

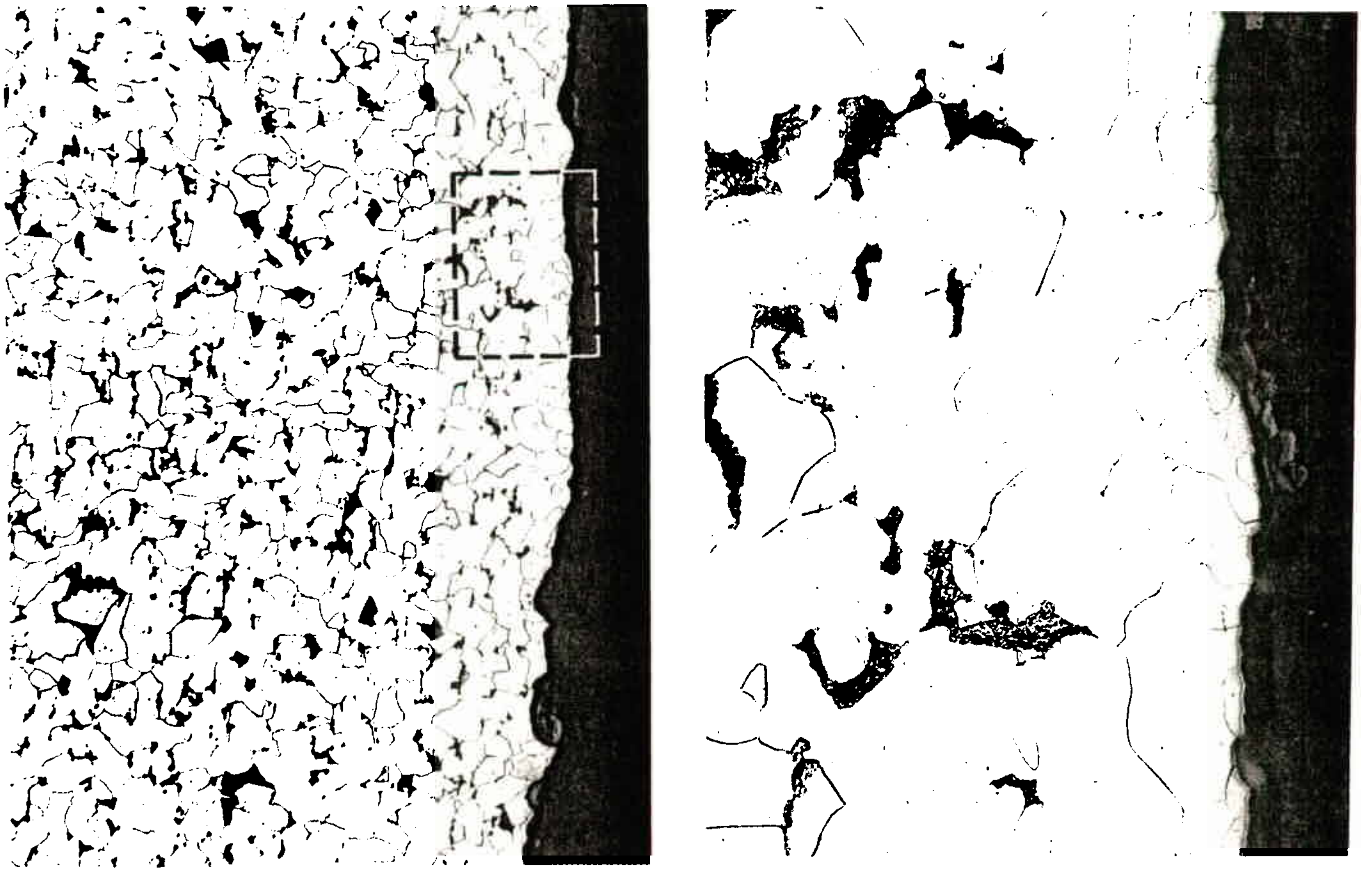

A B

Figure 14. Microstructure At "A_4" (100X) (500X).

A B

Figure 15. Microstructure At "A_5" (100X) (500X).

Figure 16. Overall View of Cross Section "B-B".
Rockwell B. Hardness Determinations Are Also Provided. Brinell Values Are Shown in ( ).
1. 53.7 (99)
2. 53.0 (98)
3. 53.) (98)

A

B

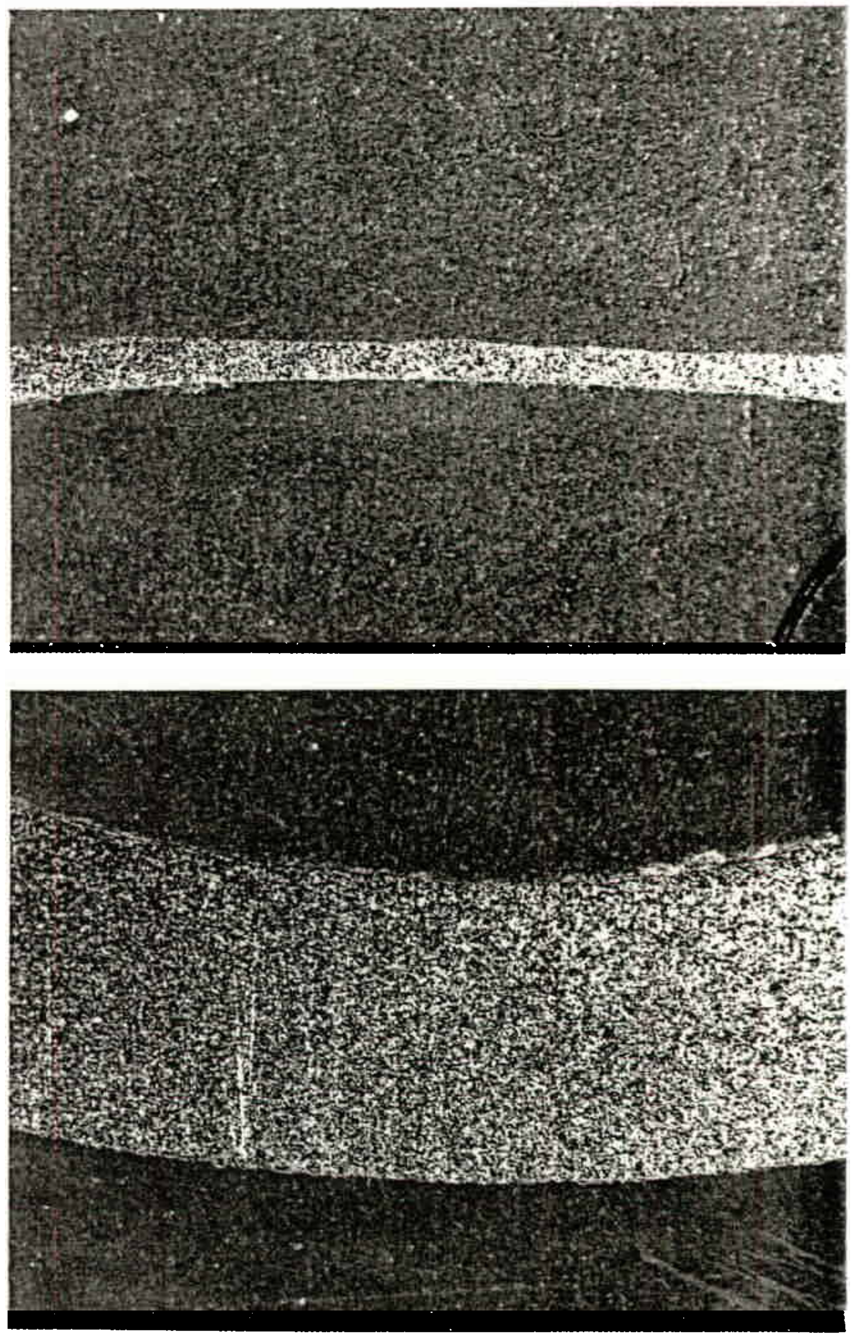

Figure 17. Photomacrograph Of Cross Section "B-B" (10X).

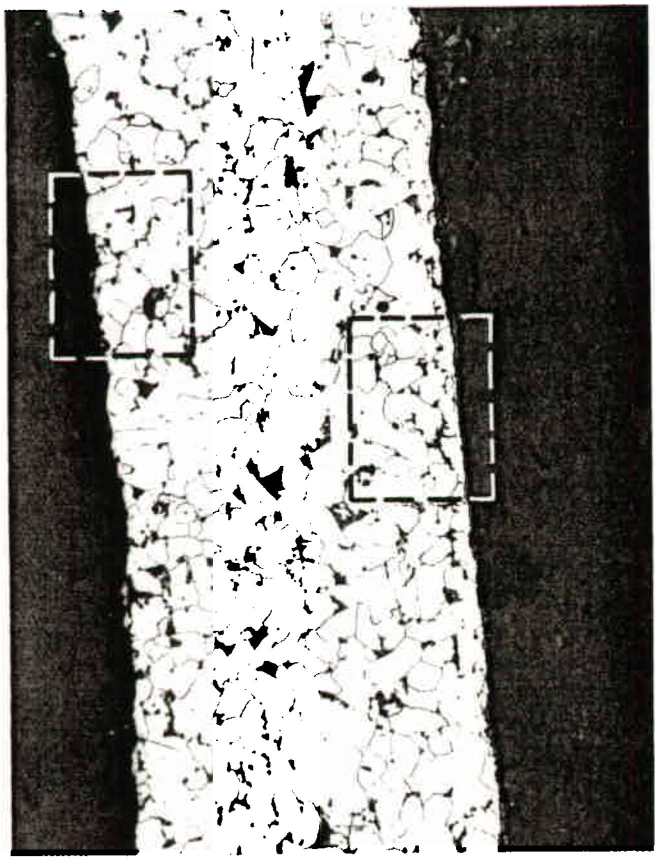

A

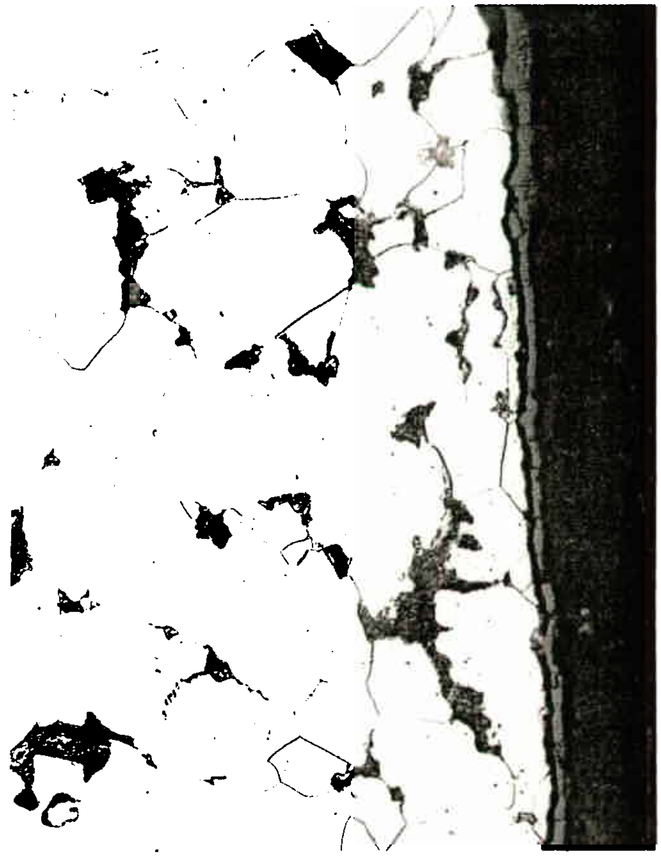

B

C

Figure 18. Microstructure At "B_2"(100X) (500X).

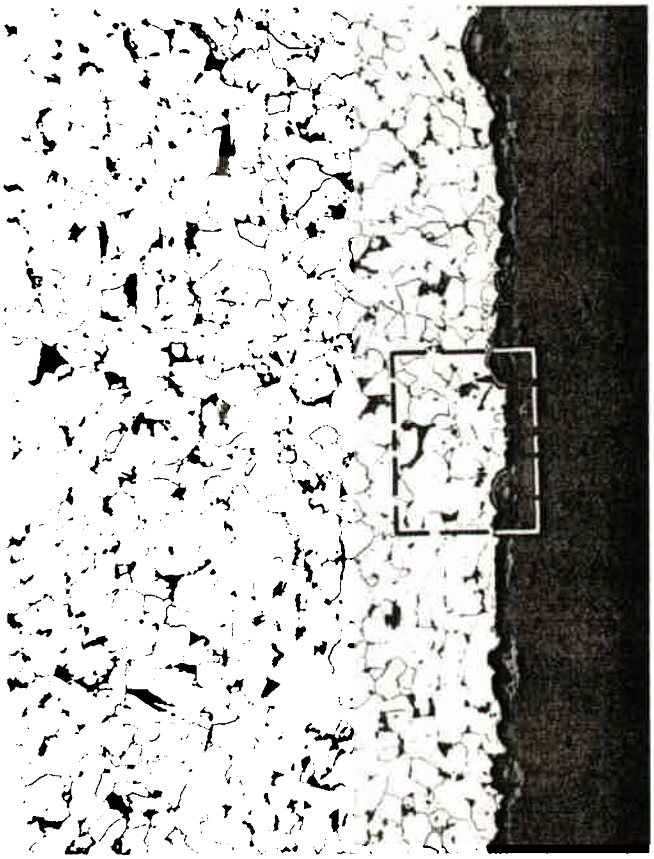

A B

Figure 19. Microstructure At "B_3" (100X) (500X).

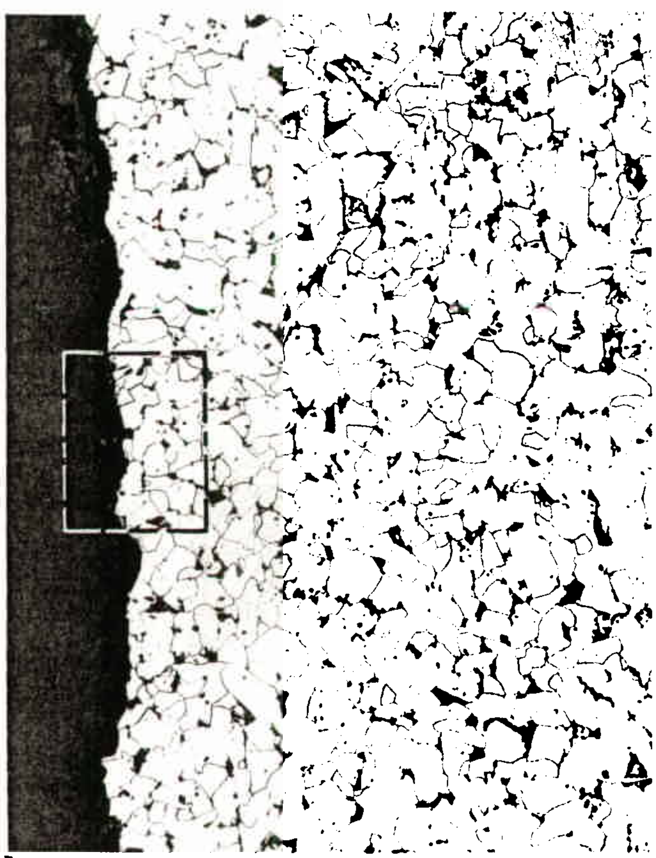

A B

Figure 20. Microstructure At "B_4" (100X) (500X).

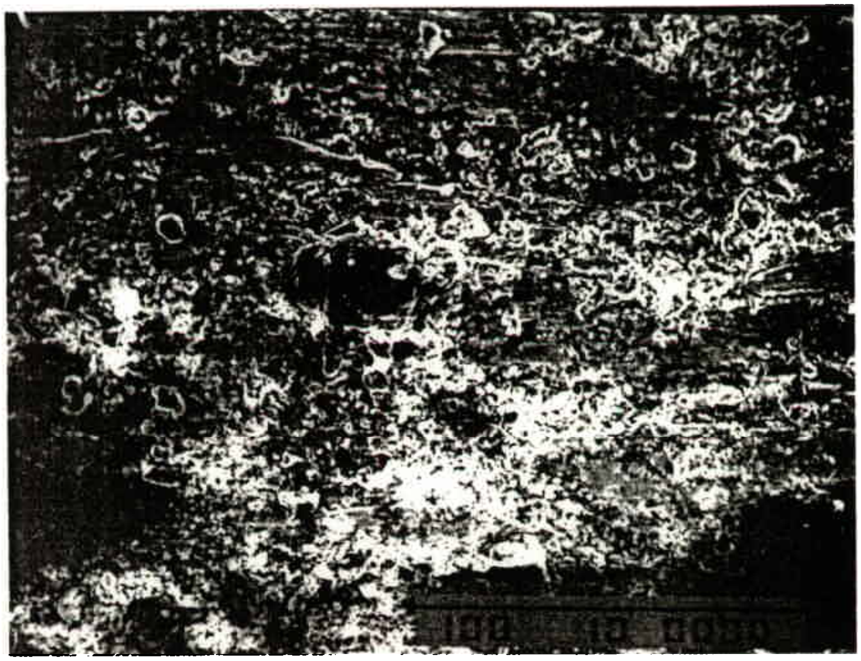

Figure 21. Scanning Electron Micrograph (SEM) At Location "C".

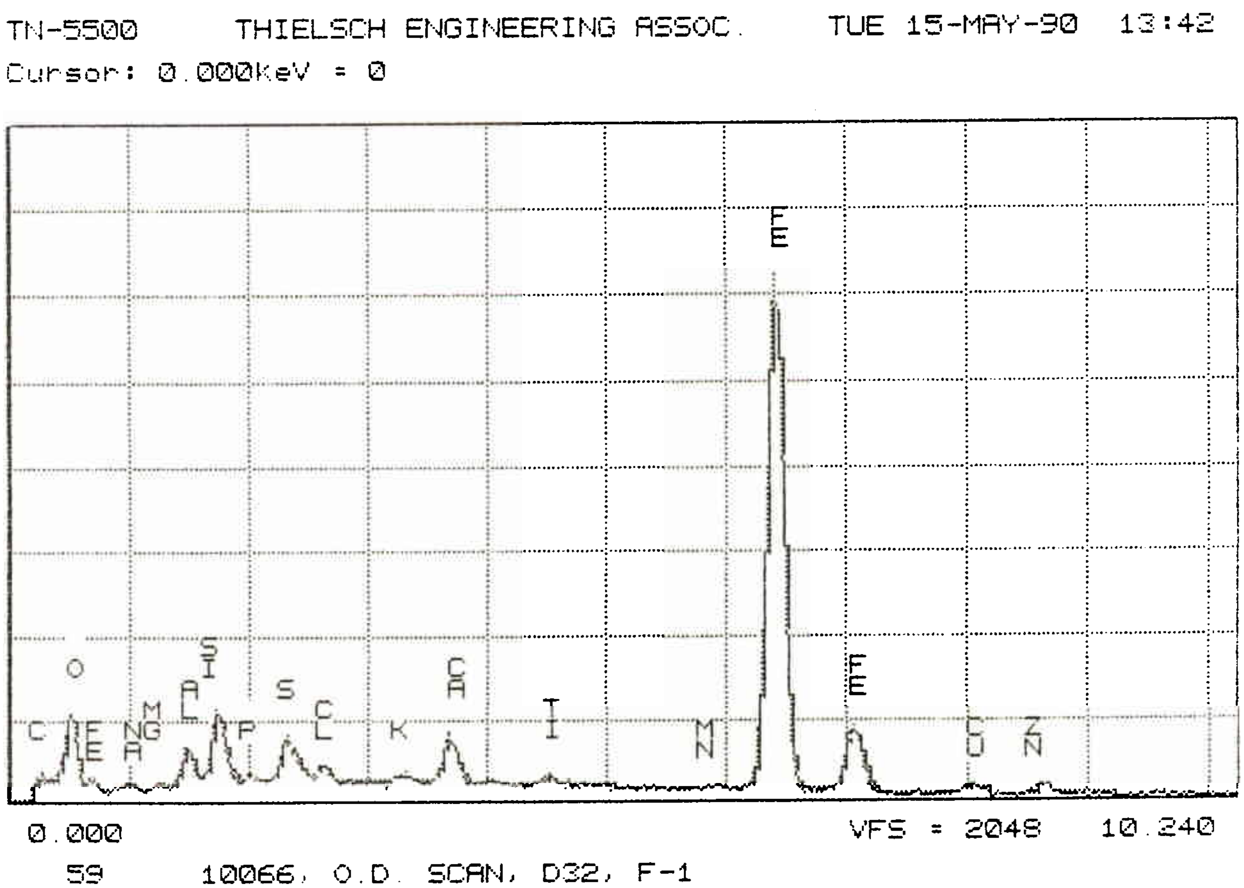

Figure. 22. Energy Dispersive Spectral (EDS) Plot At Location "C".